Assessing comparability and uncertainty of analytical methods for methylated mercury species in seawater

Alina Kleindienst, Igor Živković, Emmanuel Tessier, Alkuin Koenig, Lars-Eric Heimbürger-Boavida, Milena Horvat, David Amouroux

Assessing comparability and uncertainty of analytical methods for methylated mercury species in seawater

Alina Kleindienst[1]*, Igor Živković[2,3], Emmanuel Tessier[1], Alkuin Koenig[4], Lars-Eric Heimbürger-Boavida[5], Milena Horvat[2,3], David Amouroux[1]*

[1]Université de Pau et des Pays de l'Adour, E2S UPPA, CNRS, IPREM, Institut des Sciences Analytiques et de Physico-chimie pour l'Environnement et la Matériaux, Pau, France

[2] Department of Environmental Sciences, Jožef Stefan Institute, Jamova cesta 39, 1000 Ljubljana, Slovenia

[3] Jožef Stefan International Postgraduate School, Jamova cesta 39, 1000 Ljubljana, Slovenia

[4] Univ. Grenoble Alpes, CNRS, INRAE, IRD, Grenoble INP, IGE, 38000 Grenoble, France

[5]Aix Marseille Université, CNRS, IRD, Univ. Toulon, Mediterranean Institute of Oceanography (MIO), 13288 Marseille, France

*Corresponding authors. A. Kleindienst, D. Amouroux

Address: IPREM CNRS/UPPA, Technopôle Helioparc, 2 Av. du Président Pierre Angot, 64053 Pau, France

E-mail: akleindienst@univ-pau.fr, david.amouroux@univ-pau.fr

Phone : +33 559407756

Submitted to Analytica Chimica Acta June 2023

Highlights:

- We investigated the measurement uncertainty for direct and indirect methylated mercury species in seawater
- Species specific isotope dilution calibration improve significantly the uncertainty budget
- Comparable results for methylated mercury species between indirect and direct measurements
- Lower uncertainty obtained for indirect dimethylmercury measurements, except below 50 fM

Keywords:

Methylated Mercury, Speciation measurements, Dimethyl Mercury, Monomethyl Mercury, Uncertainty, Comparability

Graphical abstract:

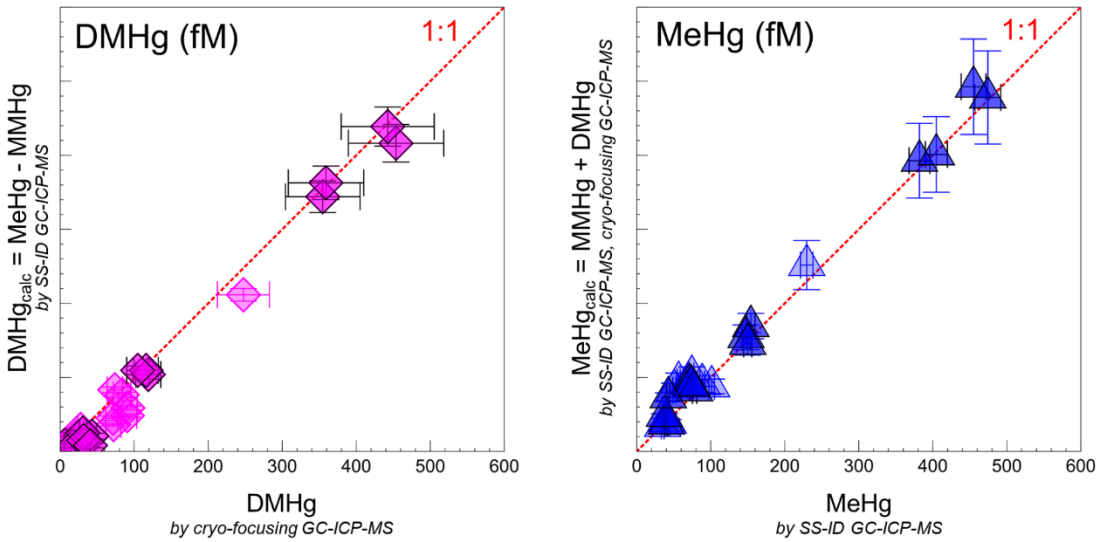

Abstract

Background: The relative distribution and importance of monomethylmercury (MMHg) and dimethylmercury (DMHg) in seawater is still under debate. A lack of comparability between measurements at sub-picomolar levels hampered the further understanding of the biogeochemical Hg cycle. To overcome this, we assessed the relative standard measurement uncertainties ($U_{ex,r}$) for direct measurements of MMHg and DMHg by species-specific isotope dilution ICP-MS and cryo-focusing GC-ICP-MS at femtomolar concentrations. Furthermore, $U_{ex,r}$ was determined for the indirect determination of DMHg ($DMHg_{calc}$ = MeHg - MMHg) and MeHg ($MeHg_{calc}$ = MMHg + DMHg) to compare the two methodologies.

Results: Expanded $U_{ex,r}$ (confidence interval of 95%) for cryo-focusing GC-ICP-MS was 14.4 (< 50 fM) and 14.2% (> 50 fM) and for SS-ID GC-ICP-MS and 5.6 (< 50 fM) and 3.7% (> 50 fM). For concentrations above 50 fM, $U_{ex,r}$ for $DMHg_{calc}$ was always lower than for direct measurements (14.2%). For $MeHg_{calc}$, on the other hand, $U_{ex,r}$ was always higher for concentrations above 115 fM (range: 3.7-13.9%) than for direct measurements (3.7%). We then evaluated the comparability of directly measured and calculated DMHg and MeHg concentrations based on Hg speciation measurements for two vertical profiles in the Mediterranean Sea. We show that directly measured and indirectly determined DMHg and MeHg concentrations yield comparable results.

Significance: Our results validate the application of the indirect method for the determination of DMHg if a direct measurement method with a low $U_{ex,r}$ such as isotope dilution is used for MMHg and MeHg measurements. The validation of the indirect measurement approach opens new possibilities to generate more precise and accurate DMHg data in the global ocean.

1 Introduction

Mercury (Hg) is a toxic element, ubiquitous in seawater at very low levels (~ 1 pM) and known to biomagnify in the aquatic food web as monomethyl-Hg (CH_3Hg^+, hereon MMHg). It is of concern for wildlife and humans since MMHg toxicity can lead to neurological damage [1]. Humans are exposed to MMHg primarily through the consumption of seafood [2]. The most common Hg-species known to be present and of importance in seawater are inorganic Hg(II), dissolved gaseous elemental Hg (Hg(0)), MMHg and dimethyl-Hg ($(CH_3)_2Hg$, hereon DMHg) and various transformation pathways between Hg-species exist [3]. Much progress has been made concerning the environmental factors that drive MMHg concentrations and distribution in the environment [4–7]. However, our understanding of the origin and fate of methylated-Hg species (MeHg = MMHg + DMHg) in seawater is still limited by analytical difficulties regarding their precise and accurate determination at femtomolar levels (MeHg typically below 600 fM) [7]. The comparability of analytical and sampling methodologies (e.g. filtration) applied by different laboratories also requires further assessment [8,9]. Indeed, one of the goals of the Minamata Convention (stated in Article 19) is the harmonization of methodologies for data collection to improve data comparability for all Hg-species.

While MMHg is mostly present in the dissolved or particulate form binding various ligands, DMHg is present as a dissolved neutral gaseous form [10,11]. Since its first determination in seawater [12], DMHg has been shown to be ubiquitous in the marine environment. Upon acidification, DMHg decomposes into MMHg [13], such that total MeHg can be detected as MMHg [14,15]. While this approach is convenient and widely used [8], valuable information on the relative importance and distribution of both MeHg species is lost. Separate quantification of both species can be achieved through the degassing and trapping of DMHg before sample preservation and subsequent analysis of DMHg (trap) and MMHg (water). However, due to the volatility and potential instability of DMHg, species separation should be done within hours of sampling [16], and carefulness is needed to produce accurate results, from sampling, pre-concentration, and storage until analysis.

Since this method for DMHg analysis has first been established [17], few analytical studies have focused on its further development, for example by investigating alternative traps, trapping efficiency, or storage conditions [18–22]. Adsorbents used in environmental studies for DMHg in seawater are Tenax [10,23–25], Bond Elut [26,27] and Carbotrap [12,13,28–31]. Whereby only Bond Elut (Bond Elut ENV) and Carbotrap (Carbotrap®B) have been shown to be suitable to quantitively trap DMHg [19,21]. Another method developed for trapping volatile metal species in water [18], successfully applied for DMHg separation and preconcentrating, is physical trapping *via* cryogenic traps [18,32,33]. While this method limits the decomposition of DMHg, it requires more technical skills and is less convenient due to the need for liquid nitrogen. While all the formerly mentioned methods also trap Hg(0), only cryogenic traps do so quantitatively. Thus, a chromatographic separation of DMHg and Hg(0) is necessary prior to detection. Shipboard measurements are commonly performed by pyrolytic combustion and cold vapor atomic fluorescence spectrometry (CV-AFS). Detection by inductively plasma mass spectrometry (ICP-MS) can only be applied for laboratory-based measurements.

Independently of the applied method for direct DMHg detection, it is necessary to perform an external calibration. Several studies have used DMHg for calibration [17,24,25]. However, because of the instability and toxicity of DMHg, calibration is most commonly achieved through the injection of Hg(0), or less commonly by using alkylated MMHg standards [30,34]. If Hg(0) is used for calibration, known volumes of Hg(0) saturated air are injected and the quantity of injected Hg(0) is calculated based on the saturated Hg concentration in air as a function of temperature. The empirically determined Dumarey equation is commonly used for this calculation, although others have been proposed [35,36], and differences of up to 8% between approaches have been reported in literature [37]. In any case, until now, there exists no species-specific traceable certified reference material available for calibration purposes, be it for DMHg, Hg(0) or MMHg.

Analysis of MMHg from aqueous samples is commonly achieved by conversion of MMHg *via* a derivatization reaction into a volatile compound, GC separation, and detection by CV-AFS or ICP-MS

[38]. First measurements of MMHg at low environmental levels were achieved by direct ethylation [20] and hydride generation followed by cryogenic-focusing pyrolysis and AFS [39]. Unfortunately, these methods were prone to produce biased results due to matrix effects, mostly by inducing artifact formation of Hg(0) which resulted in incomplete recoveries [40]. Another drawback of these methodologies is that they rely exclusively on external calibration. Standard addition, which improves the analytical performance, results in an increase in the analytical workload and needed sample volume. An alternative to these conventional standard addition methods for MMHg analysis is offered by species-specific isotope dilution [41]. This method employs species-specific enriched stable isotopic tracers which, acting as internal standards, allow to correct for recovery, matrix effects, and potential species transformations during sample preparation [42]. Consequently, species-specific isotope dilution analysis by capillary GC-ICP-MS (SS-ID GC-ICP-MS) results in a significant improvement in the precision of MMHg measurements in aqueous samples, if compared to external calibration for ethylation and propylation GC-ICP-MS. In addition, it allows to determine Hg(II) simultaneously in the same sample analysis [43] and correct for analytical artifact formation. However, it has been shown that demethylation and methylation occurring during sample preparation is low (< 2%) in natural seawater and the artifact formation Hg(0) does not bias the results [41,44].

Several studies have reported DMHg or MeHg concentrations in seawater that were determined indirectly, i.e. calculated from direct measurements of the other two species ($DMHg_{calc}$ = MeHg - MMHg; $MeHg_{calc}$ = DMHg + MMHg) [10,26,30,45–47]. However, such methods have neither been thoroughly validated nor has the associated measurement uncertainty been assessed or the comparability between directly measured vs calculated data been established.

Measurement uncertainty is crucial for meaningful comparisons within and between studies, but unfortunately rarely adopted for observational data. Relative expanded measurement uncertainty for DMHg in seawater according to ISO/GUM Guidelines, has not previously been addressed. For MMHg, an expanded relative uncertainty of 15.8-19% and 11.1-21.3% has been reported for measurements

by direct ethylation and hydride generation, respectively. No such estimate exists for MMHg by SS-ID GC-ICP-MS in seawater. Although commonly reported in literature, relative expanded uncertainty has never been assessed for DMHg or MeHg indirectly obtained (i.e. calculated) from direct measurements of the other species (from here on indirect quantification or calculated concentrations).

Our work aimed to critically evaluate current and applicable measurement methodologies for methylated Hg-species and to investigate the comparability between direct measurements and indirect quantification for DMHg and MeHg. We determined the expanded relative measurement uncertainty for two established methods for MeHg species analysis: cryo-trapping GC-ICP-MS (DMHg) after carbotrap collection and thermal desorption and SS-ID GC-ICP-MS (MMHg) after aqueous phase propylation. Based on the obtained expanded relative measurement uncertainties of these direct measurement methodologies we established expanded relative combined standard uncertainty for the indirect quantification of $DMHg_{calc}$ = MeHg (SS-ID GC-ICP-MS) – MMHg (SS-ID GC-ICP-MS) and $MeHg_{calc}$ = DMHg (cryo trapping GC-ICP-MS) + MMHg (SS-ID GC-ICP-MS)at environmentally relevant concentrations. Finally, as a case study, we compared results for DMHg and MeHg obtained *via* direct measurements and indirect quantification for data from two profiles and one coastal station, measured in October 2020 and May 2021 in the Mediterranean Sea.

2 Material and methods

2.1 Sampling

Seawater was sampled in the Mediterranean Sea, on board of the RV Antedon II in October 2020 (shelf station, Île-Riou) and May 2021 (marginal station, K2), and from a continuous seawater intake at the Endoume coastal station (October 2020; SI Figure S1). All samples (n=23) were taken unfiltered and following trace metal clean protocols from Teflon-coated GOFLO water samplers (General Oceanic, USA). Sampling bottles made of PFA/FEP (Nalgene, ThermoFisher Scientific, USA) were thoroughly cleaned and dried under a laminar flow hood before each campaign (two consecutive 10% (v/v) HNO_3 and one 10% (v/v) HCl baths) [48]. Sample aliquots for DMHg and MeHg (analyzed as MMHg) were taken separately, according to established protocols. All sampling containers were rinsed three times with the respective sample and then filled to the top without any headspace and avoiding bubbles. Subsamples for DMHg analysis were sampled first in order to avoid the potential loss into the GOFLO sampler headspace. All samples were then stored dark and cold in double PE zip-sealed bags for transport. Pre-concentration was done within 12 h after sampling to minimize loss and inter-conversion of volatile DMHg. According to a previous study, Teflon and glass bottles are equally suitable for the storage of DMHg samples, if stored cool and dark for less than 24 h [16].

2.1.1 Sample handling and pre-concentration

A general overview of the workflow is given in Figure 1. Samples for MeHg analysis (as MMHg) were acidified using HCl (Optima™, Fisher Chemical™) to a final concentration of 0.5% (v/v) within 6 h of sampling. Custom-made traps packed with graphitized carbon (Carbotrap®, Supelco), an adsorbent previously shown to be suitable for DMHg pre-concentration [19,21,17], were used for pre-concentration (in the following carbotrap). Details on the carbotrap columns are given in the SI (Figure S2, section 2). Prior to sampling campaigns carbotrap columns were desorbed for 1 min under a

constant 100 mL min^{-1} Ar or He gas stream at 250°C for cleaning, sealed with Teflon caps and stored under a laminar flow hood, in double PE zip-sealed bags.

Pre-concentration was achieved by carefully displacing approximately 50 mL sample to form sufficient headspace. Thereafter the sampling container with approximately 450 mL of remaining sample was immediately connected to a two-way PFA transfer closure equipped with a Teflon frit (Verrerie Villeurbannaise, France) allowing the formation of fine bubbles. The seawater sample was then purged with pre-purified N_2 at ~450 mL min^{-1}, while being protected from light. Purge time was estimated (30 min) based on previous studies [49,50], to be sufficiently long (30x Sample Volume) to efficiently displace DMHg. The gas stream was dried by a cold trap before DMHg was trapped in the carbotrap column. Drying the gas stream is of major importance since previous studies indicated that moisture retained on traps lowers trapping efficiency or promotes degradation during storage [19,21]. The cold trap consisted of a home-made U-shaped glass tube containing multiple internal glass tips (Vigreux fractionating column, add 1.6 cm ID, 38 cm length) and maintained at -20°C in a Stainless-Steel Dewar (10.16 cm ID, Cole Parmer). The cold trap was prepared by placing ice cubes in ethanol or acetone. The gas flow and the temperature of the moisture trap were thoroughly checked for each sample. To assess the tightness of the system and monitor potential clogging of the cold trap due to inner ice formation. Loaded carbotraps were removed from the purging line and sealed with Teflon caps, packed in double PE zip-sealed bags. Carbotraps were stored in the dark at -20°C until analysis using cryo-focusing GC-ICP-MS. The exact sample volume was determined by comparing the remaining sample in the PFA/FEP bottle to a calibrated flask. The remaining sample (MMHg) was acidified using ultrapure HCl (OptimaTM, Fisher ChemicalTM) to a final concentration of around 0.5% (v/v). All water samples were stored in double PE zip-sealed bags at 4°C until analysis by species-specific isotope dilution and capillary GC-ICP-MS (ICP-MS, XSeries 2 Thermo Scientific).

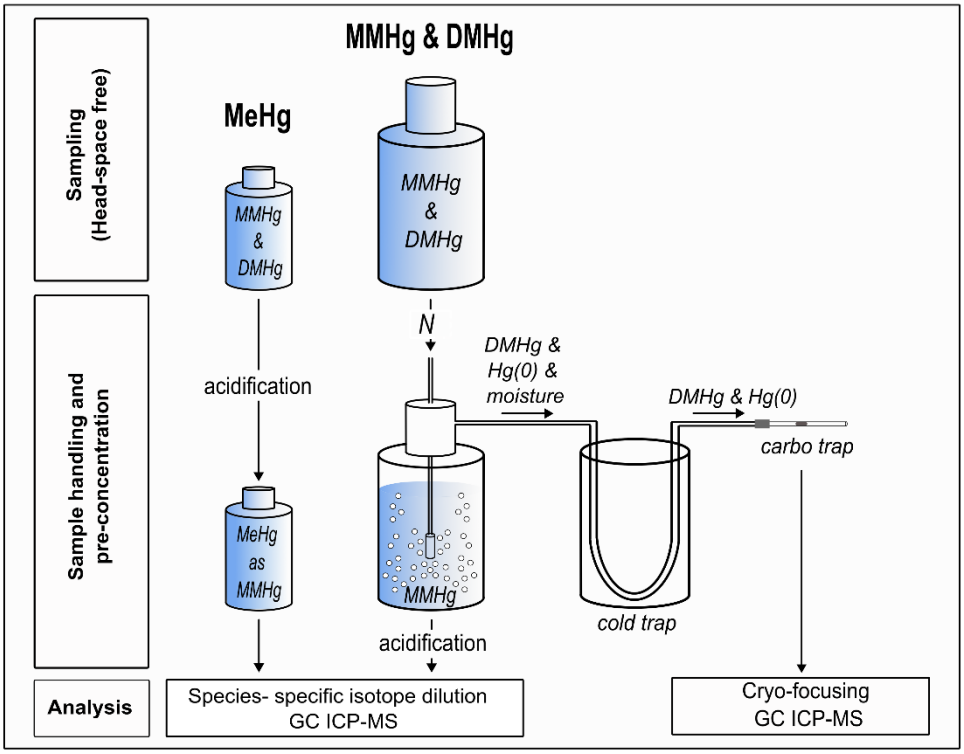

Figure 1. The general work-flow for sample handling and pre-concentration for total methylated Hg (MeHg), monomethyl Hg (MMHg) and dimethyl Hg (DMHg), and the respective analytical method.

2.2 Analysis

2.2.1 Determination of DMHg by cryo-focusing GC-ICP-MS

Carbotraps were analyzed for DMHg within 30 days of sampling and pre-concentration followed established methods [18,51]. In brief, carbotraps were connected to the chromatographic column (immersed in liquid nitrogen) and flash desorbed in a tubular oven at 250°C for 1 minute followed by 1 minute of cooling under a continuous He flow (100 mL min^{-1}). Desorption and separation of the volatile Hg compounds was realized by removing the column from the liquid nitrogen and by subsequently heating the column to 250°C (total time 5 min). Impurities in the carrier gas flow (He) are removed by passing it over a carbotrap and Au-coated sand trap. Hg(0) and DMHg elute separately and are introduced into the plasma through a heated (120°C) transfer line. Two typical chromatograms for cryo-focusing GC-ICP-MS are given in the SI (Figure S3). External calibration of the detector was achieved by injecting known quantities of Hg(0) saturated air using a gas-tight 25 or 50 µL syringe (Hamilton, USA) through a septum. The Hg(0) was pre-concentrated onto the cooled packed GC column and analysis proceeded as previously described for samples. The achieved R^2 for the linear correlation for 7 calibration points was 0.999 (SI Figure S4). Hg(0) can be used for calibration since both compounds are quantitatively trapped on the column and efficiently ionized in the plasma and thus have the same sensitivity [22]. This was confirmed with a cross calibration between Hg(0) and DMHg. Small quantities of an in-house DMHg standard (calibrated against ethylmethylmercury) were injected through a heated injector (120°C) using a calibrated micro syringe. The relative difference between the calibration coefficient for Hg(0) and DMHg was 0.6%. Details on cryo-focusing GC-ICP-MS parameterization and the calibration are presented in the SI (Table S1). No certified reference material is available, due to the volatile nature, toxicity and instability of the compound. Chromatographic peak integration was done manually with PlasmaLab (Thermo Scientific).

Blanks of DMHg were regularly checked but not observable on carbotrap columns. Desorption efficiency from carbotraps was checked by performing a second desorption step roughly every second

sample. Desorption efficiency, herein reported as the signal obtained from the first desorption relative to the sum of the signal of the first and second desorption, was 100 ± 0.3% (n = 10). Replicate analyses on separately sampled aliquots were done for two sampling points (RSD = 7% at 113 fM, n=3; RSD = 19% at 35 fM, n=3). For this method, the limit of detection (LOD) derived from background equivalent concentration calculation, was 0.06 and 0.08 pg L^{-1} (0.32 and 0.38 fM), the limit of quantification (3.3 x LOD) was 0.21 and 0.25 pg L^{-1} (1.1 and 1.25 fM) for Île-Riou and K2 samples, respectively.

2.2.2 Determination of MMHg by SS-ID GC-ICP-MS

Seawater samples were analyzed within 30 days of sampling following established methods using SS-ID GC-ICP-MS [43,44,52,53]. All reagents were prepared with ultrapure water obtained from a Milli-Q system (Millipore, 18.2 MΩ cm) and using analytical grade reagents. All working standard solutions were gravimetrically prepared in 1% HCl (Optima™, Fisher Chemical™) using an analytical micro balance (Sartorius, Germany) to a precision of 10^{-5} g. Around 100 mL of sample was weighted into acid-cleaned 125 mL glass vials with a Teflon lined cap and amended with known masses of a species-specific isotopically enriched standard solutions (spikes) (^{199}IHg, MM^{201}Hg; ISC-Science, Oviedo Spain). The optimal ratio for $^{202/201}$Hg of 0.24 for MMHg was targeted for all samples [42]. Enriched inorganic Hg (^{199}IHg) was added to monitor and correct for analytical methylation, if necessary, and was not further considered in the uncertainty estimation (further considerations in SI section 6 and Figure S5).

An acetic acid (Trace metal grade, Fisher Chemical™) /sodium acetate (≥99.5% purity, Sigma-Aldrich) buffer (0.1 M at pH 3.9, 5 mL) was then added to the sample, and the pH adjusted to the optimum pH for derivatization of 3.9 [43]. This was done by monitoring the pH with a pH meter (WTW, InoLab pH 720) and the stepwise addition of concentrated ammonium hydroxide (Optima™, Fisher Chemical™). Sodium tetra-n-propyl ($NaBPr_4$, Merseburger Spezialchemikalien, Germany) was prepared at 5% (w/v) in pre-cooled ultrapure water and used for derivatization. Isooctane (150 - 200 µL, > 99% purity, Sigma-Aldrich) and $NaBPr_4$ (80 µL) were subsequently added, the sample was immediately capped, and

shaken for 20 min on an orbital shaker (KS250, IKA Labortechnik) at 400 rpm. Then, the organic phase was recovered, transferred to an injection vial, and injected in triplicates within 12 h of extraction. Operating conditions for the capillary GC-ICP-MS are given in the SI (Table S3) together with a general sample preparation scheme (Figure S6). Peak integration was done manually using PlasmaLab (Thermo Scientific). An RSD of < 2% between $MM^{202}Hg/MM^{201}Hg$ ratios was obtained and $MM^{199}Hg/MM^{202}Hg$ ratios were checked for the natural ratio expected from natural Hg abundances. Concentrations were calculated according to the classical isotope dilution formula (see Eq 3) [43].

Before every session, the concentration of the enriched isotopic spikes and the relative abundances of the Hg isotopes were determined by SS-ID GC-ICP-MS (referred to as Reverse Isotope Dilution, RID) as previously described in literature [42]. The RSD typically obtained for triplicate RID sample preparations was < 1% (at 100 and 150 ng L^{-1} $MM^{201}Hg$). Further considerations regarding the precise characterization of the enriched spike are provided in the SI (section 9). No certified reference material is available for MMHg in seawater at ambient concentrations. However, method validation has been done previously, principally through the addition of MMHg at ambient concentration or close to the limit of quantification in natural fresh- or seawater [53,44,43]. In addition, the accuracy for THg (as the sum of MMHg and iHg) has previously been verified [54]. Replicate analyses of the same sample were also performed (RSD = 5.86% at 47 fM or 9.44 pg L^{-1}, n=3). Reagent blanks were checked thoroughly but no blank correction was necessary. For this method, the LOD, derived from background equivalent concentration calculation, was 1.4 and 1.6 pg L^{-1} (7 and 8 fM) and the limit of quantification (3.3 x LOD) was 4.5 and 5.5 pg L^{-1} (22.6 and 27.2 fM) for Île-Riou and K2 samples, respectively.

2.3 Measurement uncertainty estimation

Uncertainty of measurement results was estimated for cryo-focusing GC and SS-ID following ISO GUM/Eurachem guidelines [55–57] Following these guidelines, we determined measurement uncertainty for the two analytical methods (direct measurements of compounds). Both Type A and

Type B uncertainty sources were taken into consideration when determining the combined standard uncertainties. Based on the direct measurement uncertainty we then determined the relative expanded uncertainty ($U_{ex,r}$) for DMHg and MeHg calculated by mass balance (indirect quantification). Additional information on the measurement uncertainty estimation is given in SI in Table S4.

2.3.1 Measurement uncertainty for DMHg by cryo-focusing GC-ICP-MS

The uncertainty for direct DMHg measurements was estimated using the following model equation

$$c(DMHg) = \frac{A(S) * \frac{1}{m}}{V(S)} \qquad \text{(Eq 1)}$$

where ***c*** is the concentration of DMHg in the sample to be determined, ***A(S)*** is the blank-corrected signal (area), ***m*** is the calibration coefficient determined by external calibration and ***V(S)*** is the Volume of the sample. Contributions of the uncertainty sources based on this model (Eq 1) are shown in a fishbone diagram in the SI Figure S7. Uncertainties arising from the measured temperature within the bell jar and the equation [35] used to calculate the mass of Hg(0) were included in the calibration term. Measurement uncertainty of the Dumarey equation was estimated as a type B uncertainty, assigned by the δ parameter having the value 1 and ± 8% uncertainty with a rectangular probability distribution, as previously suggested elsewhere [58]. Due to the volatile nature of the analyte and the analytical technique, repeated injection of the same pre-concentrated sample is not possible thus repeatability cannot be assessed. As peak integration was done manually, the repeatability of integration was assessed and included in *A(S)*. The relative combined standard uncertainty ($u_{r,c}$) was calculated as shown in the following equation (Eq 2) where u_r are the relative standard uncertainties of individual uncertainty sources. Blank correction was not necessary thus was not included in $u_{r,c}$.

$$u_{r,c}\big(c(DMHg)\big) = \sqrt{u_r(A\,(S))^2 + u_r(V(S))^2 + u_r(m)^2} \qquad \text{(Eq 2)}$$

2.3.2 Measurement uncertainty for MMHg by SS-ID GC-ICP-MS

Uncertainty of measurement for MMHg by SS-ID was estimated based on the following equation

$$c(MMHg) = \frac{c' w' A_r (RY' - X')}{w\, A_r' (X - RY)} \times d \quad \text{(Eq 3)}$$

where ***c*** is the concentration of MMHg in the sample to be determined, ***c'*** is the concentration of the enriched spike, ***w'*** is the mass of the enriched isotopic spike, $\boldsymbol{A_r}$ is the atomic weight of natural Hg, ***R*** is the measured ratio $MM^{202/201}Hg$ determined by ICP-MS, ***Y'*** is the abundance of the ^{201}Hg-isotope in the enriched spike, ***X'*** is the abundance of the ^{202}Hg isotope in the enriched spike, ***w*** is the mass of the sample analyzed, $\boldsymbol{A'_r}$ is the atomic weight of the enriched spike, ***X*** is the natural abundance of the ^{202}Hg isotope, and ***Y*** is the natural abundance of the ^{201}Hg isotope. Finally, a density correction for seawater samples is applied ***d***. Contributions of the uncertainty sources based on this model (Eq 3) are shown as fishbone diagram in the SI Figure S8. Significant blank contributions were not observed and therefore not included in the uncertainty budget.

The relative combined standard uncertainty ($u_{r,c}$) was calculated as shown in the following equations where u_r is the relative standard uncertainties of individual uncertainty sources. Relative standard uncertainty on *c'* was determined in a separate step in the same way for RID as shown in the following including all uncertainties related to certificated MMHg purity, preparation and dilution of the natural MMHg standard.

$$u_{r,c}(RY') = \sqrt{\left(\frac{u_R}{R}\right)^2 + \left(\frac{u_{Y'}}{Y'}\right)^2} \quad \text{(Eq 4)}$$

$$u_{r,c}(RY) = \sqrt{\left(\frac{u_R}{R}\right)^2 + \left(\frac{u_Y}{Y}\right)^2} \quad \text{(Eq 5)}$$

$$u_{r,c}\,(RY' - X') = \sqrt{u\,(RY')^2 + u\,(X')^2} / \,(RY' - X') \quad \text{(Eq 6)}$$

$$u_{r,c}(X - RY) = \sqrt{u(X)^2 + u(RY)^2} / (X - RY) \qquad \text{(Eq 7)}$$

$$u_{r,c}(c(MMHg)) =$$

$$\sqrt{u_r(c')^2 + u_r(w')^2 + u_r(A_r)^2 + u_{r,c}(RY' - Y')^2 + u_r(w)^2 + u_r(A_r')^2 + u_{r,c}(X - RY)^2 + u_r(d)^2}$$

(Eq 8)

2.3.3 Measurement uncertainty for calculated DMHg, MeHg and DMHg/MeHg

Based on the properties of DMHg and its decomposition to MMHg upon acidification [13] DMHg and MeHg can be calculated. While DMHg can be calculated by subtraction of measured MMHg from MeHg (from here $DMHg_{calc}$), MeHg can be calculated as the sum of measured DMHg and measured MMHg (from here $MeHg_{calc}$). The propagated relative combined standard uncertainty ($u_{r,c}$) was calculated for both approaches based on the relative combined standard uncertainties associated to analytical methods for the respective Hg-species as shown in the following equations:

$$u_c\big(c(DMHg_{calc})\big) = \sqrt{u(MeHg_{meas})^2 + u(MMHg_{meas})^2} \qquad \text{(Eq 9)}$$

$$u_{r,c}(DMHg_{calc}) = \frac{u_c\big(c(DMHg_{calc})\big)}{c(DMHg_{calc})} \qquad \text{(Eq 10)}$$

$$u_c\big(c(MeHg_{calc})\big) = \sqrt{u(DMHg_{meas})^2 + u(MMHg_{meas})^2} \qquad \text{(Eq 11)}$$

$$u_{r,c}\,(MeHg_{calc}) = \frac{u_c\big(c(MeHg_{calc})\big)}{c(MeHg_{calc})} \qquad \text{(Eq 12)}$$

The propagated relative combined standard uncertainty ($U_{ex,r}$) for the ratio of DMHg/MeHg was calculated for three scenarios as shown in equation 13. For scenario 1: $DMHg_{meas}/MeHg_{meas}$, scenario 2: $DMHg_{calc}/MeHg_{meas}$ and scenario 3: $DMHg_{meas}/MeHg_{calc}$ based on the relative combined standard uncertainties associated to each method used for determination of the concentration. The uncertainty is propagated as shown in the following equations:

$$u_{r,c}\left(\frac{DMHg_{xxx}}{MeHg_{xxx}}\right) = \sqrt{u_{r,c}(DMHg_{xxx})^2 + u_{r,c}(MeHg_{xxx})^2} \qquad \text{(Eq 13)}$$

where xxx stands for either directly measured (meas) or calculated (calc) DMHg or MeHg as defined for each scenario.

2.4 Monte Carlo simulation and data visualization

To assess the comparability of directly measured and indirectly obtained (calculated) concentrations, we computed linear regressions (least squares). The regression coefficients (i.e. slope and intercept) and their 95% confidence intervals were estimated with a Monte Carlo simulation [59,60] using R studio [61]. Briefly, we performed repeated (n = 100,000) random resampling of each observation within its assigned probability distribution (uncertainties for both directly measured and calculated concentrations were considered), and recalculated the linear regression. This yields a probability distribution for each regression coefficient (see SI figure S9). We use the median of this distribution as the most likely coefficient value, and the 2.5th to 97.5th percentile of the distribution to define its 95% confidence interval.

Visualizations were done with veusz [62], ocean data view [63] or Inkscape [64] and the R package "ggplot2" [65].

3 Results and Discussion

3.1 Measurement uncertainty for direct measurements

The expanded relative combined standard uncertainty ($U_{ex,r}$), approximating a 95% confidence interval, was obtained by applying a coverage factor of k = 2 for both methods at two different concentrations according to ISO/Eurochem guidelines. Figure 2 illustrates the relative contributions of the individual uncertainty sources for (A) cryo-focusing GC ($DMHg_{meas}$) and (B) for SS-ID ($MMHg_{meas}$, $MeHg_{meas}$).

3.1.1 $DMHg_{meas}$

For cryo-focusing GC, $U_{ex,r}$ is similar for lower $DMHg_{meas}$ (~30 fM) and higher $DMHg_{meas}$ (~300 fM) concentrations (14.4% and 14.2%, respectively). The external calibration accounts for the highest relative contribution to $U_{ex,r}$ (always > 97%) in both cases. At low concentrations, the repeatability of the peak integration becomes slightly more important resulting in a maximal contribution of 2.76% to $U_{ex,r}$. It has to be noted that uncertainties related to sampling, possible degradation before purging, and purge efficiency have not been included in this assessment. Our results highlight the importance and single dependency of $U_{ex,r}$ on the external calibration for direct DMHg measurements in seawater. Relative expanded measurement uncertainties for gaseous Hg-species in seawater have not previously been reported in literature. Published values for $U_{ex,r}$ for total gaseous Hg measurements in air, with similar uncertainty sources as determined in this study, are in agreement with our estimates, with a $U_{ex,r}$ of 13.9% (excluding sampling uncertainty) [58]. The determined $U_{ex,r}$ for DMHg is in agreement with replicated sampling and measurement (n = 3) of two samples with low and high concentrations (35 and 113 fM) performed in this study (RSD 19 and 7%).

3.1.2 $MeHg_{meas}$ and $MMHg_{meas}$

The $U_{ex,r}$ for MMHg using SS-ID GC-ICP-MS at lower (~30 fM) and higher concentrations (~150 fM)are 5.6 and 3.7%, respectively. Five individual sources constitute around 99% of $U_{ex,r}$, at both concentration

levels. The three highest contributions come from the abundance of $MM^{202}Hg$ of the enriched spike (*X'*), the ratio between $MM^{202/201}Hg$ (*R*) and the concentration of the enriched spike (*c'*). Minor contributions are from the natural abundance of ^{201}Hg (*Y*), and the natural abundance of ^{202}Hg (*X*) compared to the formerly mentioned sources. From the five main sources all except two, the concentration of the enriched spike and $MM^{202/201}Hg$ ratio, are certified values or are established in literature and thus cannot be improved. For low levels, the relative standard uncertainty on the $MM^{202/201}Hg$ ratio (*R*) increases from 1 to 2% due to higher variability in the integration of smaller peak areas.

The relative expanded uncertainty for MMHg in seawater at both concentration levels is lower than for a solid reference material analyzed by HPLC-Q-ICP-MS ($U_{ex,r}$ 11%) [66]. Moreover, measurement uncertainty estimations for ID-ICP-MS for other elements in solid reference materials (Cd, Cr, Pb) are in agreement with our results with $U_{ex,r}$ (k = 2) < 4% [67]. Our results highlight the relative importance of the accurate determination of the spike concentration by RID and the injection repeatability [42]. The $U_{ex,r}$ (k = 2) for the concentration of the enriched tracer (*c'*) was determined separately and was with 2.7% (k = 2) in the range of previously published values of 0.7 and 4.1% [66]. Individual uncertainty sources for the determination of *c'* by RID are illustrated in detail in the SI (Figure S10).

$U_{ex,r}$ for other commonly used methods for MMHg determination in seawater, such as hydride generation (HG, 11.1-21.3%) or direct ethylation (ET, 15.8-19-3%) followed by pyrolysis and GC-AFS, is considerably higher [68]. For both methods, the main contributions to $U_{ex,r}$ were reported to come from the standard repeatability, sample repeatability, and recovery [68]. None of these are of major importance for SS-ID GC-ICP-MS since the internal spiking method corrects for recovery, no external calibration is needed, and sample repeatability from triplicate injections is usually < 2%. The $U_{ex,r}$ estimated in this study is in the range of repeated measurements of artificial seawater spiked with MMHg of < 2% [43] and from replicates analyzed in this study with < 6%.

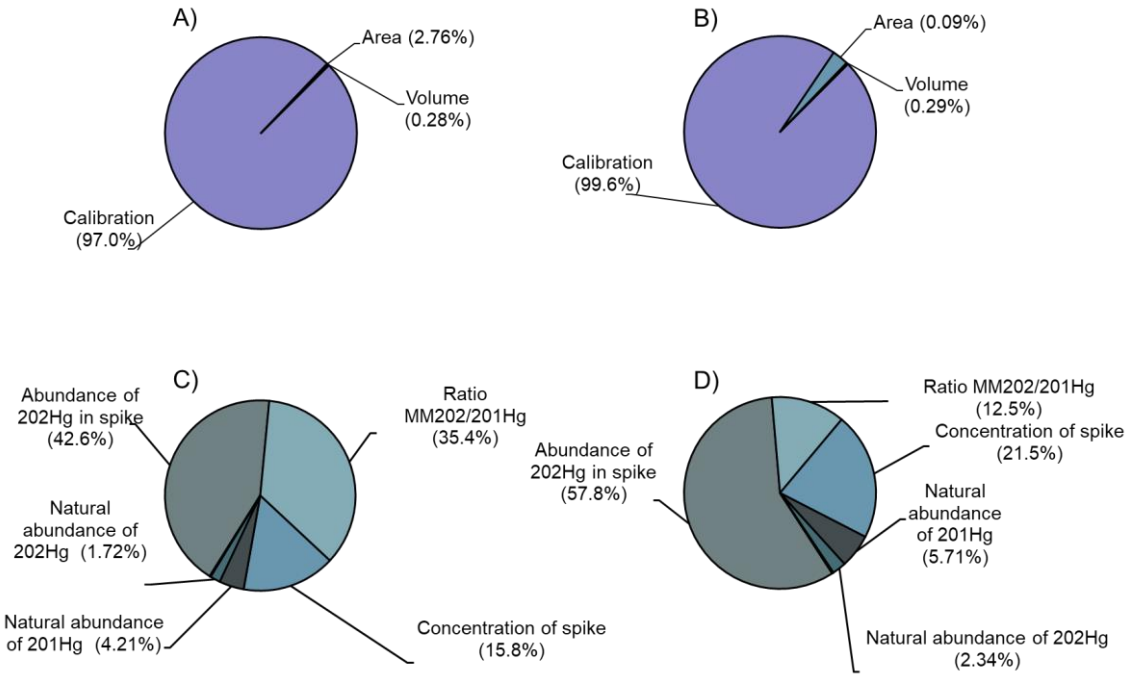

Figure 2. Relative contribution indexes (square sum of variances) for the individual uncertainty sources (in %) to the expanded relative uncertainty at low (< 50 fM) and high (> 50 fM) concentration for (A) $DMHg_{meas}$ at low concentrations with $U_{ex,r}$ = 14.4% and (B) and high concentrations with $U_{ex,r}$ = 14.2% (C) for $MMHg_{meas}$ at low concentrations ($U_{ex,r}$ = 5.6%) and (D) high concentrations ($U_{ex,r}$ = 3.7%)).

3.2 Uncertainty propagation for calculated DMHg and MeHg

Due to different analytical approaches between studies, it is common practice to calculate either DMHg or MeHg based on a mass balance approach, i.e. considering that MeHg = DMHg + MMHg [e.g. 30, 45] We assessed $U_{ex,r}$ for calculated $DMHg_{calc}$ and $MeHg_{calc}$ according to equations 9-12 for $U_{ex,r}$ determined in this study, and for $U_{ex,r}$ for hydride generation and direct ethylation based on theoretical datasets [68]. We only considered the $U_{ex,r}$ for direct DMHg measurements established in this study since no other literature data was available. Finally, we determined the $U_{ex,r}$ for calculated DMHg and MeHg for field observations with $U_{ex,r}$ from this study. The applied $U_{ex,r}$ for each analytical methodology at the respective concentration levels are summarized in Table 1.

3.2.1 Theoretical considerations

To investigate the sensitivity of $DMHg_{calc}$ and $MeHg_{calc}$ to the absolute concentration of the Hg-species involved in the calculation, we created theoretical datasets. The $U_{ex,r}$ of $DMHg_{calc}$ was determined for DMHg concentrations of up to 800 fM while maintaining MMHg concentrations constant at either 15 fM or 100 fM (thus covering the expected range of MMHg in the environment). Similarly, the $U_{ex,r}$ of $MeHg_{calc}$ was determined for MeHg concentrations of up to 800 fM, again maintaining MMHg constant at either 15 fM or 100 fM. Expected trends of $U_{ex,r}$ for $DMHg_{calc}$ and $MeHg_{calc}$ are shown in Figure 3.

Table 1. Summarized $U_{ex,r}$ for different direct measurement methodologies ([a] this study, [b]Živković et al., 2017).

	DMHg ($U_{ex,r}$ %)	MeHg or MMHg as MMHg ($U_{ex,r}$ %)		
	Cryo-focusing GC-ICP-MS[a]	Propylation SS-ID GC-ICP-MS[a]	Direct ethylation cryo-focusing GC AFS[b]	Hydride generation cryo-focusing GC AFS[b]
< 50 fM (< 10 pg L^{-1})	14.2	5.6	19.3	21.3
> 50 fM (> 10 pg L^{-1})	14.0	3.7	15.8	11.1

3.2.1.1 $DMHg_{calc}$

Independently from the analytical method used for MeHg and MMHg analysis, $U_{ex,r}$ of $DMHg_{calc}$ tends to decrease with increasing MeHg and DMHg concentrations. Higher MMHg concentrations, relative to MeHg, result in a higher $U_{ex,r}$ for DMHg (Figure 3A, B). The magnitude of $U_{ex,r}$ of $DMHg_{calc}$, on the other hand, depends substantially on the analytical method used to determine $MMHg_{meas}$ and $MeHg_{meas}$, with a $U_{ex,r}$ for $DMHg_{calc}$ in the range of 4.3-35.3% at DMHg concentrations of around 100 fM.

In case of measurements obtained by direct ethalytion, the $U_{ex,r}$ for $DMHg_{calc}$ always exceeds the $U_{ex,r}$ of directly measured DMHg ($DMHg_{meas}$). For measurements by hydride generation, the $U_{ex,r}$ for $DMHg_{calc}$ falls below the $U_{ex,r}$ for the direct DMHg measurements at DMHg concentrations of around 400 fM. Finally, if SS-ID GC-ICP-MS was used to obtain $MMHg_{meas}$ and $MeHg_{meas}$, $U_{ex,r}$ was always lower for $DMHg_{calc}$ than for directly measured DMHg in case of concentrations above 50 fM (Figure 3B).

3.2.1.2 $MeHg_{calc}$

Opposed to the trend for $DMHg_{calc}$, the $U_{ex,r}$ of $MeHg_{calc}$ increases with increasing MeHg concentrations (Figure 3C, D). Since MMHg is maintained constant, the $U_{ex,r}$ of $MeHg_{calc}$ increases with increasing DMHg concentrations, because $U_{ex,r}$ is lower for $MMHg_{meas}$ than for $DMHg_{meas}$. The $U_{ex,r}$ of $MeHg_{calc}$ is dominated by $U_{ex,r}$ of direct DMHg measurements (14.2%) resulting in only small differences for $U_{ex,r}$ of $MeHg_{calc}$ above 115 fM (3.7-16.4%) between different analytical methodologies for $MMHg_{meas}$.

In fact, the overall trends for $U_{ex,r}$ of $DMHg_{calc}$ and $MeHg_{calc}$ are controlled by the $U_{ex,r}$ of the direct measurement methods used to measure the predominant species included in the calculation ($DMHg_{calc}$: MeHg or $MeHg_{calc}$: DMHg).

3.2.2 Observational data

We determined the $U_{ex,r}$ for $DMHg_{calc}$ and $MeHg_{calc}$ for two independently measured datasets from the Mediterranean Sea. The $U_{ex,r}$ for observational data and the theoretical trend and are in good agreement falling on or below the expected trend for $U_{ex,r}$ relative to calculated $DMHg_{calc}$ or $MeHg_{calc}$ in Figure 3. This shows that it is feasible to use the calculation approach at environmentally relevant concentrations if SS-ID GC-ICP-MS is used.

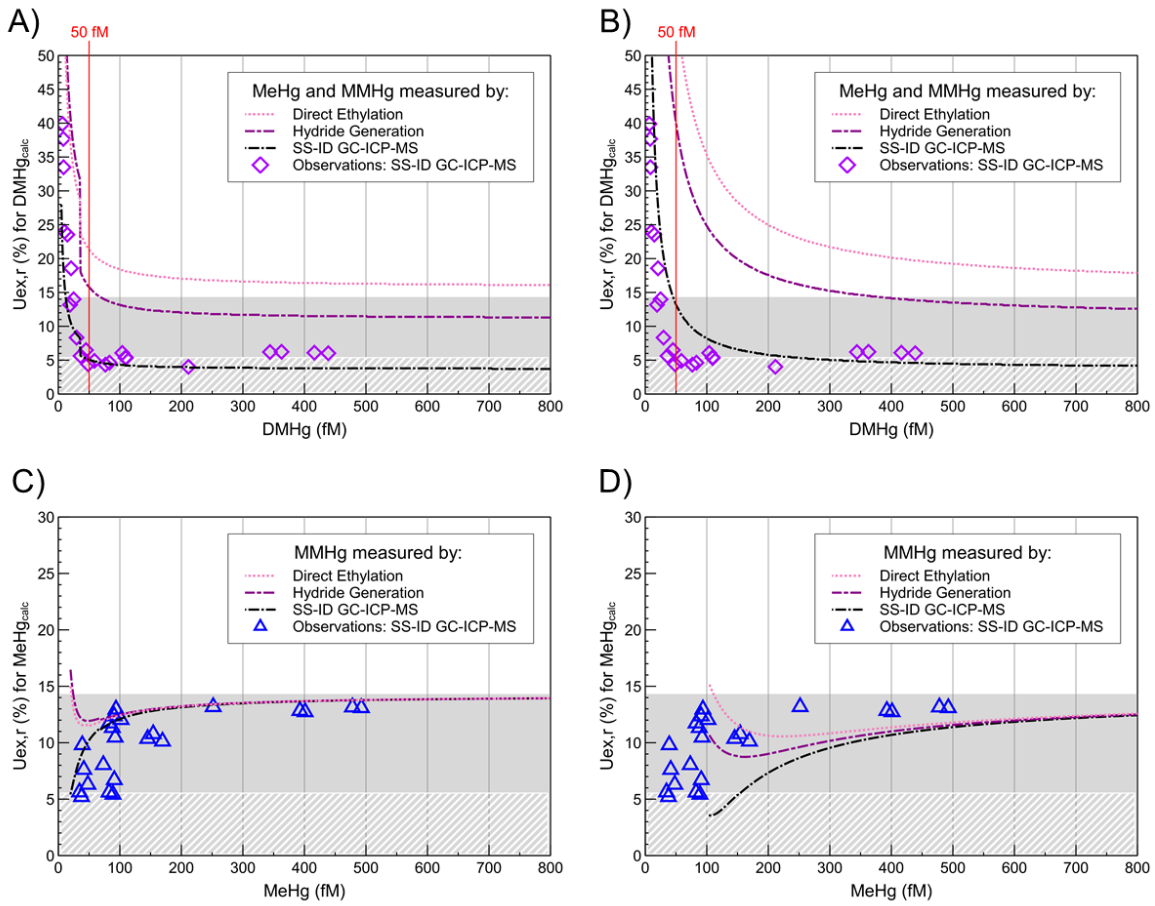

Figure 3. Illustration of calculated expanded relative uncertainty ($U_{ex,r}$) for theoretical datasets and different direct measurement methods and the subsequently calculated $DMHg_{calc}$ or $MeHg_{calc}$ concentrations. Shaded grey area indicates the $U_{ex,r}$ of direct $DMHg_{meas}$ measurements by cryo-trapping GC-ICP-MS (~14%) and white hatched area $U_{ex,r}$ for direct $MMHg_{meas}$ measurements by SS-ID GC-ICP-MS (max ~6%). Calculated $U_{ex,r}$ for observational data based on $U_{ex,r}$ for direct measurements determined in this study are indicated with diamond or triangle symbols. For variable DMHg with constant MMHg concentrations of 15 fM (A), or 100 fM (B), and MeHg at 15 fM MMHg (C), or 100 fM MMHg (D). (A, B) $U_{ex,r}$ of $DMHg_{calc}$ decreases with increasing DMHg concentrations, opposed to this trend, $U_{ex,r}$ for $MeHg_{calc}$ increases with increasing MeHg concentrations (C, D).

3.3 Comparability between direct and indirect quantification methods

3.3.1 DMHg and MeHg

Our observations for DMHg and MeHg concentrations in two vertical profiles included in this study are similar to previous measurements at the same station [47], the western Mediterranean Sea [29,69,70] and more generally in the global Ocean [8]. We compare measured and calculated concentrations of DMHg and MeHg, assigned with their corresponding relative expanded uncertainty approximating a 95% confidence interval (Figure 4). A significant linear relationship ($p < 0.001$, $n = 23$) between direct measurements and calculated concentrations can be observed for DMHg and MeHg. The slope of this linear relationship is not significantly different from 1, as confirmed by a Monte Carlo simulation (SI Figure S9). Small deviations for some datapoints from the 1:1 relationship at < 100 fM for DMHg and MeHg could be explained by a loss in precision working below the limit of quantification for measured MMHg by SS-ID GC-ICP-MS.

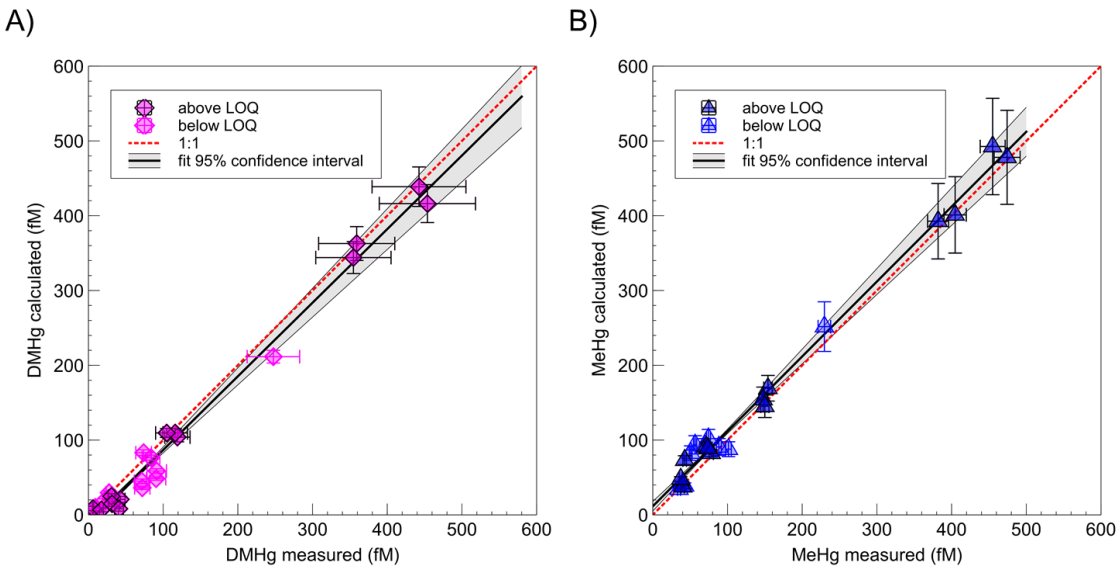

Figure 4. Correlation between measured and calculated concentrations for (A) DMHg and (B) MeHg from observational data, error bars give expanded relative uncertainty (k = 2) for the respective method and each datapoint. Light datapoints (below LOQ) indicate those datapoints in which MMHg used for calculation of calculated DMHg or MeHg was below the LOQ (23 or 27 fM). The red dotted line indicates a 1:1 relationship. The black line shows the best fit and the grey shaded area its 95% confidence interval (Monte Carlo simulation; see methods).

Relative importance of MMHg or DMHg

The ratio between DMHg/MeHg can be used to determine if DMHg constitutes an important part of the MeHg pool, as it is often the case in the subsurface global ocean [8]. Figure 5 illustrates DMHg/MeHg ratios, calculated from concentrations determined by direct or indirect measurements (Eq 13) with their $U_{ex,r}$ (k = 2) for one profile (K2 station). In scenario 1 DMHg and MeHg were directly measured, in scenario 2 MeHg was calculated, and in scenario 3 DMHg was calculated. In all three scenarios, MMHg was the dominant MeHg species to the depth of 100 m and then DMHg dominates the MeHg pool.

Figure 5. Ratio between DMHg/MeHg in one profile measured in the Mediterranean Sea and their associated relative measurement uncertainties at k = 2 for three different scenarios. scenario 1: both species were directly measured, scenario 2: MeHg was calculated from measurement data and DMHg was directly measured and scenario 3: DMHg was calculated from measurement data and MeHg was directly measured. Replicates (n = 3) were sampled and analyzed at a depth of 200 m, indicated in the black circle. Shaded area indicates region where MMHg is the predominant methylated Hg-species.

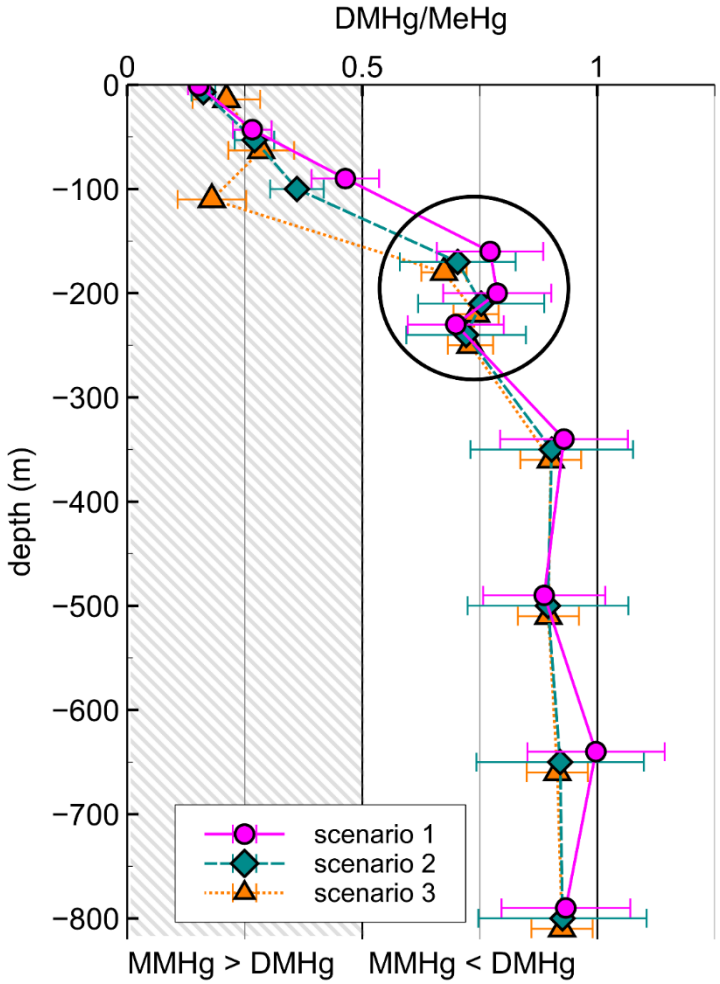

4 Conclusion

Our study confirms that the expanded relative uncertainty ($U_{ex,r}$) of SS-ID GC-ICP-MS is considerably lower than for other commonly used analytical methods for MMHg and MeHg measurements in seawater. We establish good comparability between directly measured and calculated concentrations for both DMHg and MeHg at environmentally relevant concentrations. This demonstrates that it is feasible to calculate (i.e. indirectly determine) DMHg and MeHg from measurement data if they offer good accuracy and precision (e.g. isotope dilution). This opens up the possibility to generate more DMHg observational data based on the mass balance approach and is of special interest for large oceanographic campaigns. It furthermore gives confidence in the data produced in the global ocean by different approaches. However, discrepancies observed among studies require further studies on DMHg stability, best practice for sample handling and processing methods.

Efforts have been made to apply isotope dilution for volatile Hg-species measurements to decrease the measurement uncertainty associated with the external calibration. So far, the isotope dilution approach for DMHg has only been applied at relatively high concentrations in experiments under controlled conditions in the laboratory [71–73]. Applying such an isotope dilution approach for low-level environmental samples under natural sampling conditions could further increase the accuracy of DMHg observations in seawater. However, certified traceable standards for DMHg and MMHg are needed to improve not only the comparability of MeHg measurements in seawater but also their trueness.

Competing interests' statement:

The authors declare no competing financial interests.

Acknowledgement:

We thank Natalia Torres Rodriguez (MIO), Melilotus Thyssen for access and support at Endoume (MIO) and the crew of the R/V Antedon II for support at sea. We are grateful to Bastien Duval and Océane Asensio (IPREM) for their support. This project has received funding from the European Union's Horizon 2020 research and innovation programme under the Marie Sklodowska-Curie grand agreement no. 860497 and from the Slovenian Research Agency (ARRS) through the program P1-0143.

CRediT statement

Alina Kleindienst: Conceptualization, Methodology, Validation, Investigation, Writing – Original Draft, Writing – Review & Editing

Igor Živković: Conceptualization, Methodology, Validation, Writing – Review & Editing

Emmanuel Tessier: Methodology, Validation, Investigation, Resources

Alkuin Koenig: Software, Formal analysis, Writing – Review & Editing

Lars-Eric Heimbürger-Boavida: Conceptualization, Methodology, Resources, Writing – Review & Editing, Funding acquisition

Milena Horvat: Conceptualization, Writing – Review & Editing, Funding acquisition

David Amouroux: Conceptualization, Resources, Writing – Review & Editing, Project administration, Funding acquisition

5 References

[1] S. Díez, Human health effects of methylmercury exposure, Rev Environ Contam Toxicol. 198 (2009) 111–132. https://doi.org/10.1007/978-0-387-09647-6_3.

[2] M.C. Sheehan, T.A. Burke, A. Navas-Acien, P.N. Breysse, J. McGready, M.A. Fox, Global methylmercury exposure from seafood consumption and risk of developmental neurotoxicity: a systematic review, Bull. World Health Organ. 92 (2014) 254-269F. https://doi.org/10.2471/BLT.12.116152.

[3] W.F. Fitzgerald, C.H. Lamborg, C.R. Hammerschmidt, Marine Biogeochemical Cycling of Mercury, Chem. Rev. 107 (2007) 641–662. https://doi.org/10.1021/cr050353m.

[4] T. Barkay, B. Gu, Demethylation–The Other Side of the Mercury Methylation Coin: A Critical Review, ACS Environ. Au. 2 (2022) 77–97. https://doi.org/10.1021/acsenvironau.1c00022.

[5] A.G. Bravo, C. Cosio, Biotic formation of methylmercury: A bio–physico–chemical conundrum, Limn. and Oceanogr. 65 (2020) 1010–1027. https://doi.org/10.1002/lno.11366.

[6] O. Regnell, Carl.J. Watras, Microbial Mercury Methylation in Aquatic Environments: A Critical Review of Published Field and Laboratory Studies, Environ. Sci. Technol. 53 (2019) 4–19. https://doi.org/10.1021/acs.est.8b02709.

[7] R.P. Mason, A.L. Choi, W.F. Fitzgerald, C.R. Hammerschmidt, C.H. Lamborg, A.L. Soerensen, E.M. Sunderland, Mercury biogeochemical cycling in the ocean and policy implications, Environ. Res. 119 (2012) 101–117. https://doi.org/10.1016/j.envres.2012.03.013.

[8] K.L. Bowman, C.H. Lamborg, A.M. Agather, A global perspective on mercury cycling in the ocean, Sci. Total Environ. 710 (2020) 136166. https://doi.org/10.1016/j.scitotenv.2019.136166.

[9] C.H. Lamborg, C.R. Hammerschmidt, G.A. Gill, R.P. Mason, S. Gichuki, An intercomparison of procedures for the determination of total mercury in seawater and recommendations regarding

mercury speciation during GEOTRACES cruises, LIMNOL OCEANOG-METH. 10 (2012) 90–100. https://doi.org/10.4319/lom.2012.10.90.

[10] K.L. Bowman, C.R. Hammerschmidt, C.H. Lamborg, G. Swarr, Mercury in the North Atlantic Ocean: The U.S. GEOTRACES zonal and meridional sections, Deep Sea Res. Part II Top. Stud. Oceanogr. (2015) 251–261. https://doi.org/10.1016/j.dsr2.2014.07.004.

[11] K. Bowman, C. Hammerschmidt, C. Lamborg, G. Swarr, A. Agather, Distribution of mercury species across a zonal section of the eastern tropical South Pacific Ocean (U.S. GEOTRACES GP16), Mar. Chem. 186 (2016). https://doi.org/10.1016/j.marchem.2016.09.005.

[12] R.P. Mason, W.F. Fitzgerald, Alkylmercury species in the equatorial Pacific, Nature. 347 (1990) 457–459. https://doi.org/10.1038/347457a0.

[13] F.J. Black, C.H. Conaway, A.R. Flegal, Stability of Dimethyl Mercury in Seawater and Its Conversion to Monomethyl Mercury, Environ. Sci. Technol. 43 (2009) 4056–4062. https://doi.org/10.1021/es9001218.

[14] D. Cossa, B. Averty, N. Pirrone, The origin of methylmercury in open Mediterranean waters, Limnol. and Oceanogr. 54 (2009) 837–844. https://doi.org/10.4319/lo.2009.54.3.0837.

[15] E.M. Sunderland, D.P. Krabbenhoft, J.W. Moreau, S.A. Strode, W.M. Landing, Mercury sources, distribution, and bioavailability in the North Pacific Ocean: Insights from data and models, Glob. Biogeochem. Cycles. 23 (2009). https://doi.org/10.1029/2008GB003425.

[16] J.L. Parker, N.S. Bloom, Preservation and storage techniques for low-level aqueous mercury speciation, Sci. Total Environ. 337 (2005) 253–263. https://doi.org/10.1016/j.scitotenv.2004.07.006.

[17] N. Bloom, W.F. Fitzgerald, Determination of volatile mercury species at the picogram level by low-temperature gas chromatography with cold-vapour atomic fluorescence detection, Anal. Chim. Acta. 208 (1988) 151–161. https://doi.org/10.1016/S0003-2670(00)80743-6.

[18] D. Amouroux, E. Tessier, C. Pécheyran, O.F.X. Donard, Sampling and probing volatile metal(loid) species in natural waters by in-situ purge and cryogenic trapping followed by gas chromatography and inductively coupled plasma mass spectrometry (P-CT-GC-ICP/MS), Anal. Chim. Acta. 377 (1998) 241–254. https://doi.org/10.1016/S0003-2670(98)00425-5.

[19] P.A. Baya, J.L. Hollinsworth, H. Hintelmann, Evaluation and optimization of solid adsorbents for the sampling of gaseous methylated mercury species, Anal. Chim. Acta. 786 (2013) 61–69. https://doi.org/10.1016/j.aca.2013.05.019.

[20] N. Bloom, Determination of Picogram Levels of Methylmercury by Aqueous Phase Ethylation, Followed by Cryogenic Gas Chromatography with Cold Vapour Atomic Fluorescence Detection, Can. J. Fish. Aquat. Sci. 46 (1989) 1131–1140. https://doi.org/10.1139/f89-147.

[21] N.S. Bloom, A.K. Grout, E.M. Prestbo, Development and complete validation of a method for the determination of dimethyl mercury in air and other media, Anal. Chim. Acta. 546 (2005) 92–101. https://doi.org/10.1016/j.aca.2005.04.087.

[22] C. Pécheyran, C.R. Quetel, F.M.M. Lecuyer, O.F.X. Donard, Simultaneous Determination of Volatile Metal (Pb, Hg, Sn, In, Ga) and Nonmetal Species (Se, P, As) in Different Atmospheres by Cryofocusing and Detection by ICPMS, Anal. Chem. 70 (1998) 2639–2645. https://doi.org/10.1021/ac9709615.

[23] C.R. Hammerschmidt, K.L. Bowman, Vertical methylmercury distribution in the subtropical North Pacific Ocean, Mar Chem. 132–133 (2012) 77–82. https://doi.org/10.1016/j.marchem.2012.02.005.

[24] M. Horvat, J. Kotnik, M. Logar, V. Fajon, T. Zvonarić, N. Pirrone, Speciation of mercury in surface and deep-sea waters in the Mediterranean Sea, Atmospheric Environ. 37 (2003) 93–108. https://doi.org/10.1016/S1352-2310(03)00249-8.

[25] J. Kotnik, M. Horvat, E. Begu, Y. Shlyapnikov, F. Sprovieri, N. Pirrone, Dissolved gaseous mercury (DGM) in the Mediterranean Sea: Spatial and temporal trends, Mar Chem. 193 (2017) 8–19. https://doi.org/10.1016/j.marchem.2017.03.002.

[26] A.M. Agather, K.L. Bowman, C.H. Lamborg, C.R. Hammerschmidt, Distribution of mercury species in the Western Arctic Ocean (U.S. GEOTRACES GN01), Mar Chem. 216 (2019) 103686. https://doi.org/10.1016/j.marchem.2019.103686.

[27] P.A. Baya, M. Gosselin, I. Lehnherr, V.L. St.Louis, H. Hintelmann, Determination of Monomethylmercury and Dimethylmercury in the Arctic Marine Boundary Layer, Environ. Sci. Technol. 49 (2015) 223–232. https://doi.org/10.1021/es502601z.

[28] C.H. Conaway, F.J. Black, M. Gault-Ringold, J.T. Pennington, F.P. Chavez, A.R. Flegal, Dimethylmercury in coastal upwelling waters, Monterey Bay, California, Environ. Sci. Technol. 43 (2009) 1305–1309. https://doi.org/10.1021/es802705t.

[29] D. Cossa, J.-M. Martin, J. Sanjuan, Dimethylmercury formation in the Alboran Sea, Mar. Pollut. Bull. 28 (1994) 381–384. https://doi.org/10.1016/0025-326X(94)90276-3.

[30] S. Jonsson, M.G. Nerentorp Mastromonaco, K. Gårdfeldt, R.P. Mason, Distribution of total mercury and methylated mercury species in Central Arctic Ocean water and ice, Mar Chem. 242 (2022) 104105. https://doi.org/10.1016/j.marchem.2022.104105.

[31] I. Lehnherr, V.L.S. Louis, H. Hintelmann, J.L. Kirk, Methylation of inorganic mercury in polar marine waters, Nat. Geosci. 4 (2011) 298–302. https://doi.org/10.1038/ngeo1134.

[32] M. Monperrus, E. Tessier, D. Amouroux, A. Leynaert, P. Huonnic, O.F.X. Donard, Mercury methylation, demethylation and reduction rates in coastal and marine surface waters of the Mediterranean Sea, Mar Chem. 107 (2007) 49–63. https://doi.org/10.1016/j.marchem.2007.01.018.

[33] R. Pongratz, K.G. Heumann, Determination of Concentration Profiles of Methyl Mercury Compounds in Surface Waters of Polar and other Remote Oceans by GC-AFD, Int J Environ Anal Chem. 71 (1998) 41–56. https://doi.org/10.1080/03067319808032616.

[34] K.L. Bowman, C.R. Hammerschmidt, Extraction of monomethylmercury from seawater for low-femtomolar determination, LIMNOL OCEANOG-METH. 9 (2011) 121–128. https://doi.org/10.4319/lom.2011.9.121.

[35] R. Dumarey, R. Brown, W. Corns, A. Brown, P. Stockwell, Elemental mercury vapour in air: The origins and validation of the “Dumarey equation” describing the mass concentration at saturation, Accreditation Qual. Assur. 15 (2010) 409–414. https://doi.org/10.1007/s00769-010-0645-1.

[36] M.L. Huber, A. Laesecke, D.G. Friend, Correlation for the Vapor Pressure of Mercury, Ind. Eng. Chem. Res. 45 (2006) 7351–7361. https://doi.org/10.1021/ie060560s.

[37] I. de Krom, W. Bavius, R. Ziel, E.A. McGhee, R.J.C. Brown, I. Živković, J. Gačnik, V. Fajon, J. Kotnik, M. Horvat, H. Ent, Comparability of calibration strategies for measuring mercury concentrations in gas emission sources and the atmosphere, Atmos Meas Tech. 14 (2021) 2317–2326. https://doi.org/10.5194/amt-14-2317-2021.

[38] D. Amouroux, F. Seby, M. Monperrus, F. Pannier, C. Mendiguchia, C. Benoit-Bonnemason, O.F.X. Donard, Chemical Species, in: Chemical Marine Monitoring, John Wiley & Sons, Ltd, 2011: pp. 101–160. https://doi.org/10.1002/9781119990826.ch5.

[39] P.J. Craig, D. Mennie, N. Ostah, O.F.X. Donard, F. Martin, Novel methods for derivatization of mercury(II) and methylmercury(II) compounds for analysis, Analyst. 117 (1992) 823. https://doi.org/10.1039/AN9921700823.

[40] T. Stoichev, D. Amouroux, R.C.R. Martin-Doimeadios, M. Monperrus, O.F.X. Donard, D.L. Tsalev, Speciation Analysis of Mercury in Aquatic Environment, Appl Spectrosc Rev. 41 (2006) 591–619. https://doi.org/10.1080/05704920600929415.

[41] N. Demuth, K.G. Heumann, Validation of Methylmercury Determinations in Aquatic Systems by Alkyl Derivatization Methods for GC Analysis Using ICP-IDMS, Anal. Chem. 73 (2001) 4020–4027. https://doi.org/10.1021/ac010366+.

[42] P. Rodríguez-González, J.M. Marchante-Gayón, J.I. García Alonso, A. Sanz-Medel, Isotope dilution analysis for elemental speciation: a tutorial review, Spectrochim Acta Part B At Spectrosc. 60 (2005) 151–207. https://doi.org/10.1016/j.sab.2005.01.005.

[43] M. Monperrus, E. Tessier, S. Veschambre, D. Amouroux, O. Donard, Simultaneous speciation of mercury and butyltin compounds in natural waters and snow by propylation and species-specific isotope dilution mass spectrometry analysis, Anal Bioanal Chem. 381 (2005) 854–862. https://doi.org/10.1007/s00216-004-2973-7.

[44] M. Monperrus, P. Rodríguez-González, D. Amouroux, J. Garcia Alonso, O. Donard, Evaluating the potential and limitations of double-spiking species-specific isotope dilution analysis for the accurate quantification of mercury species in different environmental matrices, Anal. .Bioanal. Chem. 390 (2008) 655–66. https://doi.org/10.1007/s00216-007-1598-z.

[45] M.V. Petrova, S. Krisch, P. Lodeiro, O. Valk, A. Dufour, M.J.A. Rijkenberg, E.P. Achterberg, B. Rabe, M. Rutgers van der Loeff, B. Hamelin, J.E. Sonke, C. Garnier, L.-E. Heimbürger-Boavida, Mercury species export from the Arctic to the Atlantic Ocean, Mar Chem. 225 (2020) 103855. https://doi.org/10.1016/j.marchem.2020.103855.

[46] A.T. Schartup, A.L. Soerensen, L.-E. Heimbürger-Boavida, Influence of the Arctic Sea-Ice Regime Shift on Sea-Ice Methylated Mercury Trends, Environ. Sci. Technol. Lett. 7 (2020) 708–713. https://doi.org/10.1021/acs.estlett.0c00465.

[47] M. Jiskra, L.-E. Heimbürger-Boavida, M.-M. Desgranges, M.V. Petrova, A. Dufour, B. Ferreira-Araujo, J. Masbou, J. Chmeleff, M. Thyssen, D. Point, J.E. Sonke, Mercury stable isotopes constrain atmospheric sources to the ocean, Nature. 597 (2021) 678–682. https://doi.org/10.1038/s41586-021-03859-8.

[48] A.G. Bravo, D.N. Kothawala, K. Attermeyer, E. Tessier, P. Bodmer, D. Amouroux, Cleaning and sampling protocol for analysis of mercury and dissolved organic matter in freshwater systems, MethodsxX. 5 (2018) 1017–1026. https://doi.org/10.1016/j.mex.2018.08.002.

[49] M.E. Andersson, K. Gårdfeldt, I. Wängberg, F. Sprovieri, N. Pirrone, O. Lindqvist, Seasonal and daily variation of mercury evasion at coastal and off shore sites from the Mediterranean Sea, Mar Chem. 104 (2007) 214–226. https://doi.org/10.1016/j.marchem.2006.11.003.

[50] K. Gårdfeldt, X. Feng, J. Sommar, O. Lindqvist, Total gaseous mercury exchange between air and water at river and sea surfaces in Swedish coastal regions, Atmospheric Environ. (2001) 3027–3038. https://doi.org/10.1016/S1352-2310(01)00106-6.

[51] P. Pinel-Raffaitin, C. Pécheyran, D. Amouroux, New volatile selenium and tellurium species in fermentation gases produced by composting duck manure, Atmospheric Environ. 42 (2008) 7786–7794. https://doi.org/10.1016/j.atmosenv.2008.04.052.

[52] R.C. Rodríguez Martín-Doimeadios, E. Krupp, D. Amouroux, O.F.X. Donard, Application of Isotopically Labeled Methylmercury for Isotope Dilution Analysis of Biological Samples Using Gas Chromatography/ICPMS, Anal. Chem. 74 (2002) 2505–2512. https://doi.org/10.1021/ac011157s.

[53] J. Cavalheiro, C. Sola, J. Baldanza, E. Tessier, F. Lestremau, F. Botta, H. Preud'homme, M. Monperrus, D. Amouroux, Assessment of background concentrations of organometallic compounds (methylmercury, ethyllead and butyl- and phenyltin) in French aquatic environments, Water Res. 94 (2016) 32–41. https://doi.org/10.1016/j.watres.2016.02.010.

[54] A. Sharif, M. Monperrus, E. Tessier, S. Bouchet, H. Pinaly, P. Rodriguez-Gonzalez, P. Maron, D. Amouroux, Fate of mercury species in the coastal plume of the Adour River estuary (Bay of Biscay, SW France), Sci.Total Environ. 496 (2014) 701–713. https://doi.org/10.1016/j.scitotenv.2014.06.116.

[55] V.J. Barwick, S.L.R. Ellison, Measurement uncertainty: Approaches to the evaluation of uncertainties associated with recovery†, Analyst. 124 (1999) 981–990. https://doi.org/10.1039/A901845J.

[56] JCGM, 2008, Evaluation of measurement data - guide to the expression of uncertainty in measurement, https://www.bipm.org/documents/20126/2071204/JCGM_100_2008_E.pdf/cb0ef43f-baa5-11cf-3f85-4dcd86f77bd6 (last access: 23.03.2023).

[57] S.L.R. Ellison and A. Williams (Eds) Eurachem/CITAC Guide: Eurachem/CITAC guide: Quantifying Uncertainty in Analytical Measurement, http://www.eurachem.org/images/stories/Guides/pdf/QUAM2012_P1.pdf (last access: 20.12.2022)

[58] R.J.C. Brown, A.S. Brown, R.E. Yardley, W.T. Corns, P.B. Stockwell, A practical uncertainty budget for ambient mercury vapour measurement, Atmospheric Environ. 42 (2008) 2504–2517. https://doi.org/10.1016/j.atmosenv.2007.12.012.

[59] H. Janssen, Monte-Carlo based uncertainty analysis: Sampling efficiency and sampling convergence, Reliab. Eng. & Syst. Saf. 109 (2013) 123–132. https://doi.org/10.1016/j.ress.2012.08.003.

[60] N. Metropolis, S. Ulam, The Monte Carlo Method, J Am Stat Assoc. 44 (1949) 335–341. https://doi.org/10.1080/01621459.1949.10483310.

[61] R: The R Project for Statistical Computing (software). https://www.r-project.org/ (last access: 07.06.2023).

[62] Veusz – a scientific plotting package (software). https://veusz.github.io/ (last access: 07.06.2023).

[63] Schlitzer, R., Ocean Data View (software). https://odv.awi.de/ (last access: 20.10.2022).

[64] I.W. Developers, Draw Freely | Inkscape (software). https://inkscape.org/ (last access: 07.06.2021).

[65] H. Wickham, ggplot2: Elegant Graphics for Data Analysis, 2nd Edn., Springer International Publishing, Cham, 2016. https://doi.org/10.1007/978-3-319-24277-4.

[66] R. Clough, S. Belt, H. Evans, B. Fairman, T. Catterick, Investigation of equilibration and uncertainty contributions for the determinations of inorganic mercury and methylmercury by isotope dilution inductively coupled plasma spectrometry, Anal Chim Acta. 500 (2003) 155–170. https://doi.org/10.1016/S0003-2670(03)00808-0.

[67] J. Vogl, D. Liesegang, M. Ostermann, J. Diemer, M. Berglund, C.R. Quétel, P.D.P. Taylor, K.G. Heumann, Producing SI-traceable reference values for Cd, Cr and Pb amount contents in polyethylene samples from the Polymer Elemental Reference Material (PERM) project using isotope dilution mass spectrometry, Accred Qual Assur. 5 (2000) 314–324. https://doi.org/10.1007/s007690000146.

[68] I. Živković, V. Fajon, D. Tulasi, K. Obu Vazner, M. Horvat, Optimization and measurement uncertainty estimation of hydride generation–cryogenic trapping–gas chromatography–cold vapor atomic fluorescence spectrometry for the determination of methylmercury in seawater, Mar Chem. 193 (2017) 3–7. https://doi.org/10.1016/j.marchem.2017.03.003.

[69] D. Cossa, J. Knoery, D. Bănaru, M. Harmelin-Vivien, J.E. Sonke, I.M. Hedgecock, A.G. Bravo, G. Rosati, D. Canu, M. Horvat, F. Sprovieri, N. Pirrone, L.-E. Heimbürger-Boavida, Mediterranean Mercury Assessment 2022: An Updated Budget, Health Consequences, and Research Perspectives, Environ. Sci. Technol. 56 (2022) 3840–3862. https://doi.org/10.1021/acs.est.1c03044.

[70] L.-E. Heimbürger, D. Cossa, J.-C. Marty, C. Migon, B. Averty, A. Dufour, J. Ras, Methyl mercury distributions in relation to the presence of nano- and picophytoplankton in an oceanic water column (Ligurian Sea, North-western Mediterranean), Geochim. Cosmochim. Acta. 74 (2010) 5549–5559. https://doi.org/10.1016/j.gca.2010.06.036.

[71] S. Jonsson, U. Skyllberg, E. Björn, Substantial Emission of Gaseous Monomethylmercury from Contaminated Water-Sediment Microcosms, Environ. Sci. Technol.. 44 (2009) 278–83. https://doi.org/10.1021/es9020348.

[72] T. Larsson, W. Frech, Species-specific isotope dilution with permeation tubes for determination of gaseous mercury species, Anal Chem. 75 (2003) 5584–5591. https://doi.org/10.1021/ac034324s.

[73] J. West, S. Gindorf, S. Jonsson, Photochemical Degradation of Dimethylmercury in Natural Waters, Environ. Sci. Technol. 56 (2022) 5920–5928. https://doi.org/10.1021/acs.est.1c08443.